SECONDARY HYDRIDING EXPERIMENTS AND SIMULATION ON ZR-1%NB CLADDINGS

E. KOZSDA-BARSY, K. KULACSY, Z. HÓZER, M. HORVÁTH, Z. KIS, B. MARÓTI, I. NAGY, R. NAGY, T. NOVOTNY, E. PEREZ-FERÓ, A. PINTÉR-CSORDÁS, L. SZENTMIKLÓSI

Centre for Energy Research, Hungarian Academy of Sciences (MTA EK)
H-1525 Budapest, P.O. Box 49.

ABSTRACT

During LOCA (Loss of Coolant Accident) the sign of pressure difference on the two sides of cladding is reversed and the atmosphere is oxidative due to the steam. Subsequently the ballooning, burst and double-sided oxidation of the cladding can occur. Not only the oxygen but also the hydrogen can have an effect, it can diffuse into the alloy, making it brittle. In order to understand the behaviour of the cladding under these circumstances, secondary hydriding experiments were conducted in MTA EK. The alloy that was the subject of these experiments is the sponge-based Zr-1%Nb. We analysed the on-line measured data and the results of post-test examinations. And we have written a stand-alone program that contains the high temperature oxidation kinetics (mass gain and oxide layer growth) of such cladding. Simulations were made for all the experiments, and the experimental data was used for evaluation.

1. Introduction

During LOCA (in pressurised water reactors - PWRs) the pressure drops because of the leakage in the coolant pressure boundaries thus making steam formation and increase in temperature possible. These circumstances lead to the high-temperature steam oxidation of the cladding. Moreover, when the difference between the rod inner pressure and the reactor cooling system pressure becomes high enough the cladding may balloon and burst. Then the inner surface also reacts with the steam, resulting in secondary (inner surface) oxidation and hydriding. The importance of better understanding this process lies in anticipating the changes of the mechanical properties of the cladding. Studies have shown that during LOCA with increasing oxidation and hydrogen uptake zirconium alloys become more brittle [1,2,3,4]. The high temperature secondary hydriding of nuclear fuel claddings consists of several chemical, mechanical, heat and mass transfer phenomena. The ballooning creates a special geometrical arrangement in the fuel rod. The thinning of the cladding wall significantly reduces the mechanical load bearing capabilities of the tube. At high burnup the fuel pellet can fragment as it was observed in several experiments [11,12]. The temperature increase can significantly enhance fission gas release from the pellet. At the time of the burst the internal overpressure is instantaneously relieved by the release of helium and fission gases from the fuel and the pressure in the rod remains equal to the system pressure in the reactor. Gas flow out of the breach continues because of thermal expansion and fission gas release. The gas outflow may essentially suppress the internal oxidation, and this partially explains the rather limited area of internal oxidation around the breach [13].

In order to support the safe operation of VVER reactors in Hungary, the secondary hydriding phenomenon was investigated in a recent experimental series with E110 type claddings, which is a zirconium alloy used in VVER reactors. The E110 has different variants, but the basis is zirconium with a 1% niobium content. Niobium is known to reduce oxidation and hydrogen absorption in zirconium [3,4]. The high-temperature behaviour of two varieties of cladding under LOCA conditions was tested at the Hungarian Academy of Sciences Centre for Energy Research (MTA EK) [6]. The E110 alloy is in use today at Paks NPP, while E110G (sometimes referred to as sponge-based E110 Opt) is a new development. The fabrication process of E110G differs from that of the E110 alloy: instead of the electrolytic

refinement it is fabricated from sponge zirconium, which also leads to a lower level of hafnium and halogens.
The present study covers post-test examinations performed following earlier secondary hydriding tests in MTA EK [6], providing further data on E110G behaviour. The objectives of this study are extending the secondary hydriding test results with data on VVER type cladding behaviour and comparing the E110G alloy to its predecessor E110. In addition, numerical simulations were also carried out to evaluate the measured results.

2. Materials and methods

2.1. Experimental approach

The main purpose of the experiments was to simulate LOCA (loss-of-coolant accident) conditions in order to understand the behaviour of the cladding during such events. Furthermore, it had to meet the following criteria: possible comparison between E110 and E110G samples (similar circumstances), large crack after burst, oxidation for different durations (to analyse time dependence), modelling purposes and possible comparison to results of similar tests performed in other laboratories.
The experiments were not aimed at being completely representative of real LOCA conditions but were focused on the investigation of selected phenomena under well-defined conditions. The rather complex temperature and pressure histories were represented in a simplified way applying linear pressurisation rate and isothermal burst and oxidation conditions. The two step experiments (similarly to the CEA tests [5]) were selected for the following reasons:

- The prevention of oxidation in the ballooning and burst phase results in larger deformation and opening [15]. The rods were intended to have a large opening in order to enhance the penetration of steam into the inner volume of the sample in the oxidation phase.
- The experimental data supports the numerical modelling. The separation of oxidation and burst phenomena allows the code developers to improve their models individually for the burst and for the oxidation process without interference.

The burst of E110 claddings in oxidizing atmosphere with typical transient conditions was investigated in another test series with electrically heated fuel rod bundles in the CODEX (Core Degradation EXperiment) facility [14]. The post-test examination of the CODEX-LOCA bundles provided additional data on the mechanical properties, oxygen and hydrogen distribution in the cladding tubes and will be compared to the secondary hydriding results.
Two types of as-received Zr-1%Nb cladding samples were used, provided by the Russian fuel supplier: E110 and E110G. The composition of these materials is presented in Table 1. The measurements were made by spark ionisation source mass spectrometer (type MS-702R).

	Nb	Mg	Al	Si	Cr	Mn	Fe	Ni	Cu	Hf
E110G	10000	1.5	10	35	30	5	500	15	5	10
E110	10000	0.5	0.5	1	10	0.1	45	15	0.5	100

Table 1. Material composition of the Zr-1%Nb samples (in weight ppm)

The samples used in the secondary hydriding tests were 300 mm long with an inner diameter of 7.73 mm and outer diameter of 9.1 mm. They were filled with inert Al_2O_3 pellets.

2.2. Experimental setup

The experimental setup included means to control the temperature and inner pressure of the rod. It provided sufficient steam flow for the oxidation to occur, and argon flow to carry the steam or to slowly cool down the samples. Quenching with water was also possible. The experimental facility consisted therefore of two loops. In the first (ballooning and burst) loop high purity argon gas was used, controlled by a stepper motor through a needle valve, and connected to the inner volume of the sample situated in the resistance-type tube furnace. The second loop was for the oxidation of the rod and the quenching. Its components were a

steam generator, another high purity argon tank, a precision pump and a thermal conductivity detector (TCD). The schematics of the setup is presented in Figure 1.

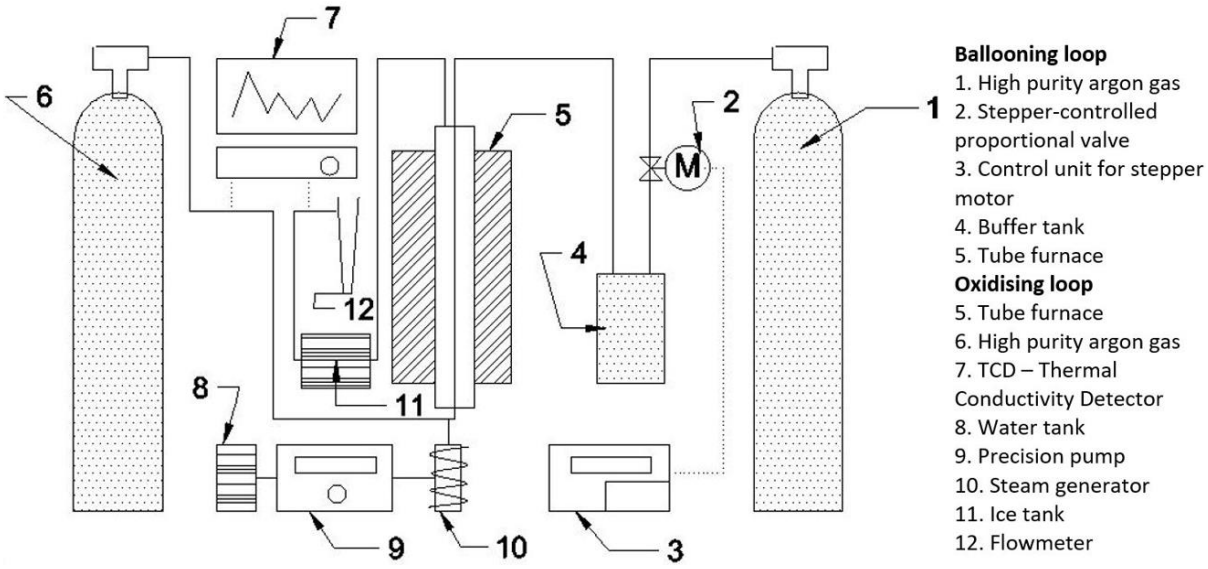

Figure 1. Schematics of the experimental loops (the dotted lines represent data transfer while the solid lines represent material transfer)

A thermocouple was in the 10 mm gap between the sample and the wall of the furnace, at the thermal centre of the furnace. The required temperature was regulated with the feedback of this thermocouple.

2.3. Experimental procedures

The secondary hydriding experimental programme conducted at MTA EK included eleven successful tests [6]. Some of the samples were broken during the oxidation phase or during handling of the cladding tubes after the tests. For this reason, only eight samples were available for further examinations. The estimated ECR (equivalent cladding reacted) values indicated here have been calculated using an average ballooned diameter of 20 mm along with the relevant best-estimate oxidation kinetic correlations at the thermal centre. The ECR results are therefore more realistic for the tested alloys than those calculated using either the Cathcart-Pawel or the Baker-Just correlations.

Sample name	refE110	refE110G	ESH1	GSH12	GSH22	GSH42	GSH52	GSH62*
Cladding type	E110	E110G	E110	E110G	E110G	E110G	E110G	E110G
Burst temperature (°C)	800	800	800	800	800	800	750	800
Oxidation temperature (°C)	-	-	1000	1000	1000	1150	1150	1000
Oxidation duration (s)	-	-	200	200	1200	300	120	1200
Estimated ECR (%)	-	-	7.8	6.8	14.7	26.4	16.7	14.7

*quenched sample

Table 2. Test matrix of the examined samples (the reference rods were not oxidised)

Steps	Tasks	Measured parameters
Calibration	- Calibration of the TCD - Furnace T profile measurements	T (thermocouple), hydrogen cc (TCD)
Heating	- Heating of the cladding until the central region along the axis reaches T_{burst} - From 20 °C to 750/800 °C at 1 bar, Ar atmosphere	T, p (manometer)
Pressurising (Ballooning and burst)	- Increasing the inner pin pressure by 0.08 bar/s - Ballooning and burst of the sample	T, p, flow rate (bubble flow meter
Heating	- Heating up to T_{ox} - From 750/800 °C to 1000/1150 °C	T
Oxidation (Secondary hydriding)	- Steam flow of 0.66 g/s - Oxidation times vary between 120-1200 s	T, flow rate, hydrogen cc
Cooling	- Slow cooling: 7 l/min Ar gas - Quench: water flooding	T, flow rate, hydrogen cc
PTEs	- Geometry, metallography, PGAA, hot vacuum extraction, 4-point bending, SEM-EDX	-
Simulation	- T profile corrections - Oxide layer thickness - Oxide mass increase - Volume of released hydrogen	-
Evaluation	Comparison of experimental and calculated values: - Oxide layer thickness - Volume of released hydrogen	-

Table 3. Steps of the test procedure and parameters measured on-line

The tests started at room temperature (20 °C), the sample was inserted into the furnace and fastened in the thermal centre (both axially and radially) and the argon flow was started. The furnace heating was turned on and kept on for approx. 20 minutes, until the thermal centre of the furnace reached the desired ballooning temperature (750-800 °C). After a short equilibration time the pressurisation by argon started. The gas was supplied until the burst happened, typically between 4.5-5.5 MPa, then the pressurisation was stopped.
As the next step, the furnace was heated to the temperature of the oxidation, the TCD was connected to the system and the steam generator was switched on. During the oxidation of the cladding the temperature rose due to the exothermic reaction, but it was not significant (4-7 °C) because the steam and argon flow transported most of the excess heat.
In the cooling phase the steam supply and the heating were turned off, the argon flow was increased and the TCD still kept going in order to detect the stagnant hydrogen still leaving the furnace.

2.4. Post-test examinations (PTEs)

First, the non-destructive analysis was carried out on two of the cladding tubes. The hydrogen to zirconium ratio was measured by prompt gamma activation analysis (PGAA). The advantage of this technique is the high sensitivity for light elements, in this study hydrogen, because of the favourable difference between the neutron cross sections of the H and Zr (H: 0.3326 b; Zr: 0.185 b). The variation in the atomic ratio of these two elements was therefore measured axially.

Then all the tubes were submitted to mechanical testing. Four-point bending technique was used to test the flexural strength of the samples. Both oxidised and reference (ballooned-only) samples were tested in order to make comparisons.
After the mechanical tests, sample preparation was needed for the other examinations. First, the sample pieces (the ones that were broken during the four-point bending) were placed back into their original positions and cast with a two-component resin and different sections were cut.
Then long sections (15 mm) were used for microscopic analysis (metallography). With the use of a Reichert Me-F2 optical microscope the grain structure was examined at two different resolutions. The thin sections (3 mm) were used for hydrogen content (hot extraction) measurements. The results were in good agreement with the PGAA, therefore the latter was used further on.
Several cladding tubes were prepared for scanning electron microscopy (SEM). The SEM was coupled with an energy-dispersive X-ray spectroscope (EDX). The atomic composition of the samples was examined by an Iridium X-ray Fluorescence (IXRF) EDX.

2.5. Simulations

As part of the cross-checking process, a standalone Fortran code was written to calculate the oxidation of the E110G cladding and to estimate the amount of hydrogen generated. These values were then compared to the measurements.
As the first step, the temperature profile of the furnace was calculated using the experimental results. The time evolution of the axial temperature profile after reaching any of the constant temperatures relevant to the experiments was measured and could be approximated as

$$T = [A_s - pe^{-qt}]x^2 + T_s \quad (1)$$

where

T is the calculated temperature (°C) at a given time (t) and axial position (x),
t is the time elapsed since the central thermocouple reached the target temperature (s),
x is the distance from the thermal centre (mm),
T_s is the measured centre temperature (°C)
and

$A_s = -3 \cdot 10^{-7}T - 8.95 \cdot 10^{-3}$
$p = 8.6 \cdot 10^{-6}T - 5.32 \cdot 10^{-3}$
$q = 6.25 \cdot 10^{-7}T - 7.03 \cdot 10^{-5}$

The next step of the procedure was the calculation of cladding oxidation. New kinetic correlations have recently been established at MTA EK for the oxidation of the E110G alloy [8], these were used for the calculations (Equation 2, Table 4). For E110, previously established equations were used [7].

$$w(t,T)=k(T)\cdot t^{\alpha(T)} \quad (2)$$

where w is the oxide layer thickness (m) or mass increase per unit surface area (g/cm^2), t is the oxidation time (s), T is the temperature (K).

Model	Range	*w* *dimension*	*k*	*α*
E110G	t ≤ 500 s or 1335 K – 1473 K	m g/cm^2	$5.276 \cdot 10^{-11} e^{(7.6783 \cdot 10^{-3} \cdot T)}$ $8.678 \cdot 10^{-9} e^{(7.6783 \cdot 10^{-3} \cdot T)}$	0.5
	t > 500 s and 873 K – 1276 K	m g/cm^2	$8.038 \cdot 10^{-12} e^{(1.0044 * 10^{-2} \cdot T)}$ $1.322 \cdot 10^{-9} e^{(1.0044 * 10^{-2} \cdot T)}$	$0.7776 - 3.573 \cdot 10^{-4} \cdot T$
	t > 500 s and 1276 K – 1335 K	m g/cm^2	$9.407 \cdot e^{(-1.1735 \cdot 10^{-2} \cdot T)}$ $1547 \cdot e^{(-1.1735 \cdot 10^{-2} \cdot T)}$	$-3.561 + 3.042 \cdot 10^{-3} \cdot T$

Table 4. Fitted parameters of the oxidation kinetics of E110G in Equation 2 [8]

In the last step the volume of the released hydrogen was calculated.

3. Results and discussion

3.1. Ballooning and burst

Burst time (counted from the beginning of pressurisation until the burst) and the burst pressure indicate the mechanical properties of the cladding. Both quantities depend on the state of the cladding (fresh or oxidised), on temperature and on the pressurisation rate. In most cases the burst of E110 samples happened at higher pressures, for example, at 800 °C the E110 samples burst around 5.0 MPa, the E110G samples around 4.8 MPa. At lower temperature (750 °C) the burst happened later, and the claddings endured almost fifty percent higher inner pressure [6].

The samples ballooned to more than twice their original diameter (9.10 mm) at the location of burst (Figure 2). Lower temperature means higher burst pressure, as it was expected. The sizes of ballooned samples are quite similar, partly because of the similar conditions (pressurisation rate, temperature) and partly due to the similar mechanical properties of the E110 and E110G alloys. The typical length of burst openings was about 21 mm.

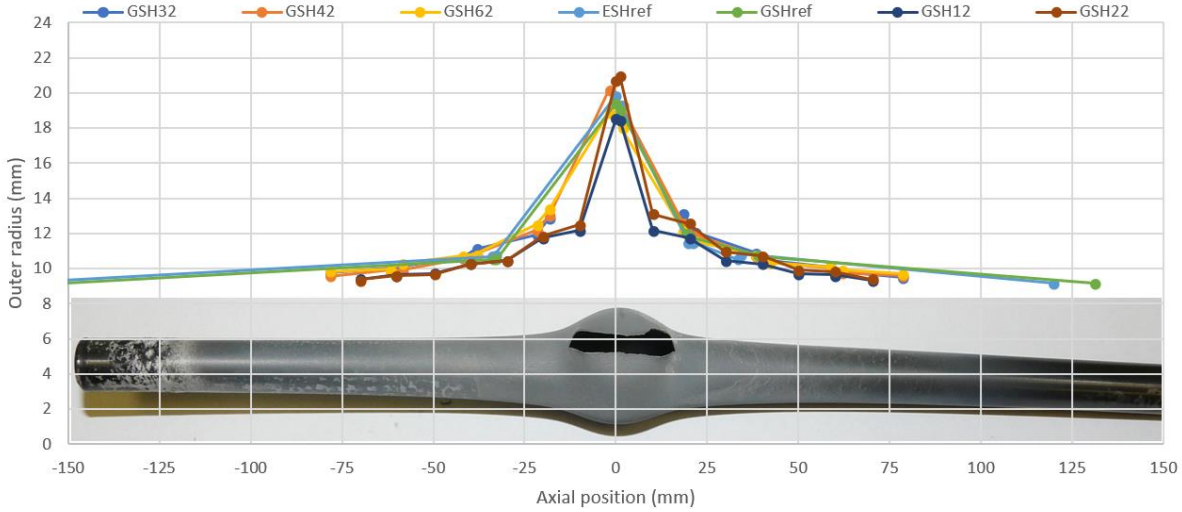

Figure 2. Geometry of rods after burst at 800 °C

3.2. Oxidation

The results obtained from EDX measurements indicate a non-uniform radial and axial distribution of the oxygen in the cladding after oxidation. The radial distribution (Figure 3) shows a high oxygen content in the oxide layer. After the oxide-metal interface (O/M) the mass ratio drops rapidly, and then slightly increases again in the metal.

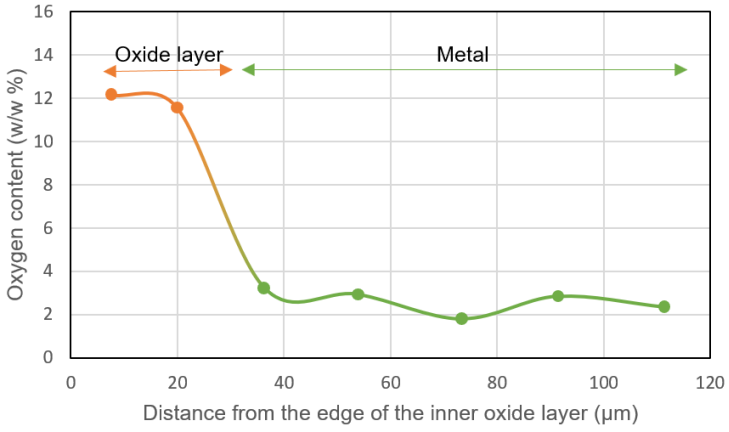

Figure 3. Radial distribution of oxygen in sample GSH52 (at axial position -18.3 mm)

In terms of the axial profile, there is a significant difference between the inner and outer oxide layers. Whilst the outer layer covers the whole rod in most cases, the inner oxide layer formed only in the vicinity of the burst opening (Figure 4) due to the flow characteristics [10] of the gas in and around the sample.

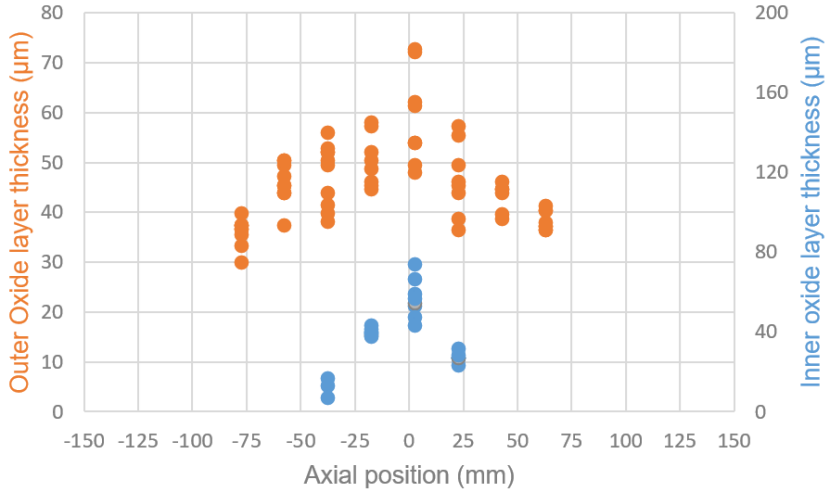

Figure 4. Measured values of inner and outer oxide layer thickness of cladding tube GSH42

Another observation was (by metallography) that the inner surface oxidation is localised within an 80-100 mm distance from the centre of burst opening. The E110G cladding tended to form a compact oxide layer (no oxide spallation occurred) (Figure 5).

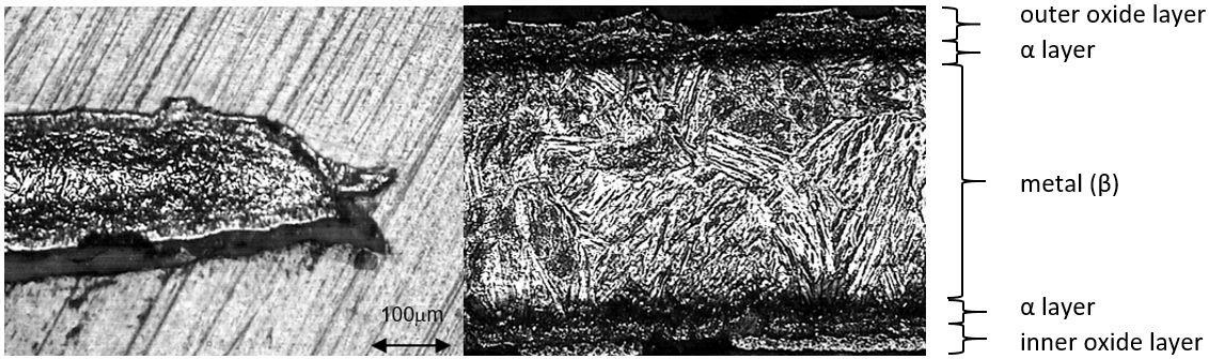

Figure 5. Inner and outer oxide layers of cladding tube GSH62 at axial position -18.3 mm

According to the four-point bending tests [6], the weakest part of the rod is the ballooned section because the cladding is thinner and more oxidised. On this section even a small force leads to fracture, contrary to the non-ballooned section. Testing of the oxidised and non-oxidised (reference) samples (Figure 6) confirmed the results of the previous mechanical tests that after the ballooning the samples still had notable flexural strength, whereas it decreased after oxidation.

The main results of the mechanical tests are as follows:

- Each sample showed signs of embrittlement, but the less oxidised samples tended to break under higher loads.
- The non-oxidised reference samples were ductile.

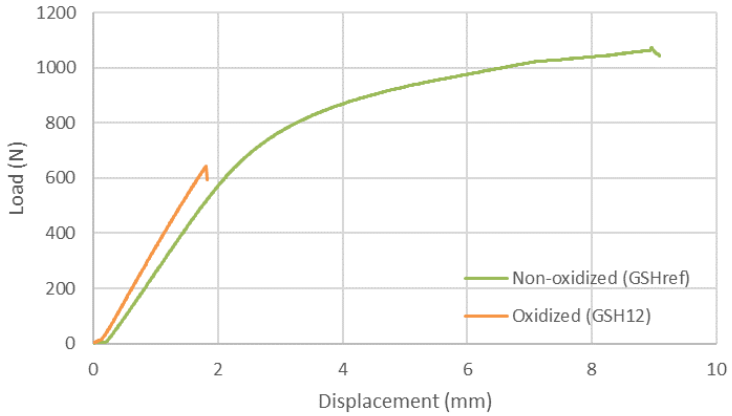

Figure 6. Four-point bending test results of oxidized and non-oxidized samples

3.3. Hydrogen absorption

Both PGAA and hot vacuum extraction indicated that the axial distribution of the absorbed hydrogen was not uniform. The highest hydrogen content (in weight percentage) is not in the burst region but a few centimetres further (the oxide layer inhibits hydrogen absorption) (Figure 7). This corresponds to other experimental results on different claddings (e.g. Zircaloy-4 [2]).

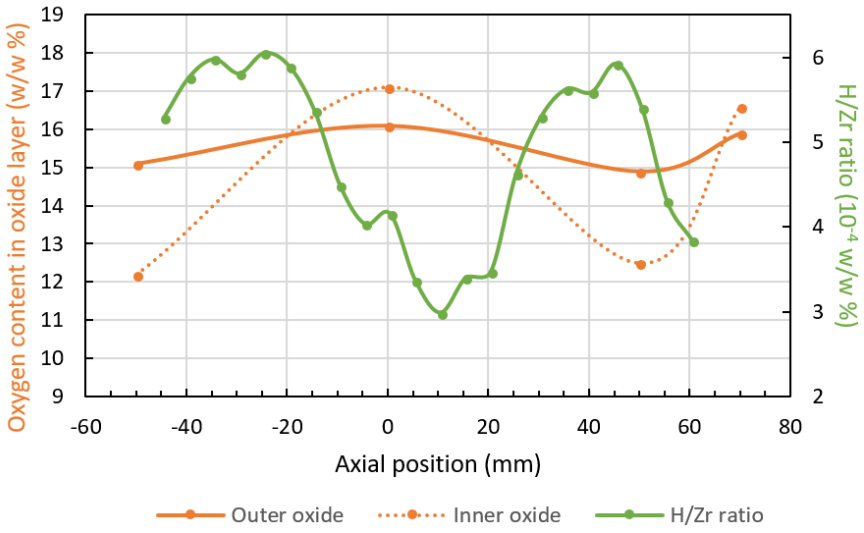

Figure 7. Axial distribution of hydrogen and oxygen in sample GSH22

3.4. Evaluation

The outer oxide layer thickness (Figure 8) was calculated to evaluate the corresponding experimental results. The correlation was R^2=0.8908 with an average difference of 5.8 µm.
The measured and calculated hydrogen release was also compared. During the oxidation of zirconium in steam, hydrogen forms according to the equation:

$$Zr + 2H_2O = ZrO_2 + 2H_2 \quad (3)$$

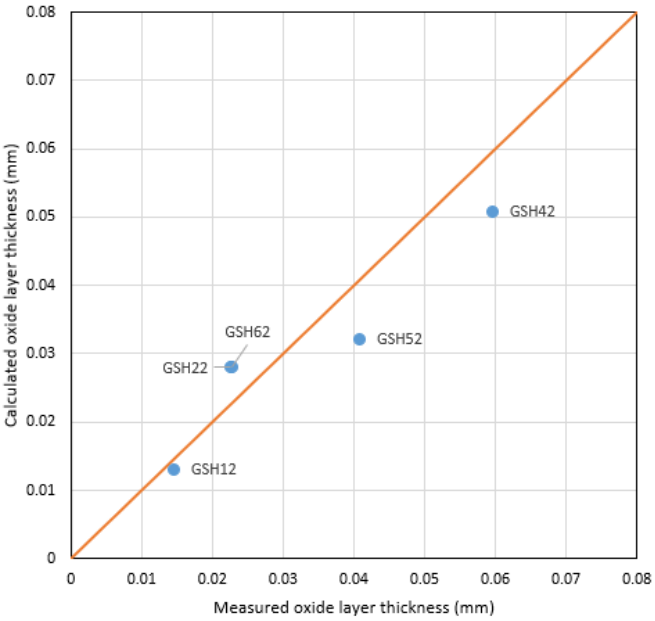

Figure 8. Experimental results compared to the simulations (outer oxide layer thickness)

Some amount of hydrogen is absorbed by the metal, while most of it is released and detected by the TCD; the sum of the released and the absorbed hydrogen equals in principle to the generated quantity. In practice, the inner geometry of the furnace affected the results – some hydrogen could not be flushed out right away, there was a build-up. As a result, there was a difference between the time distribution of the released and the detected hydrogen, so the following assumptions were applied: the temperature of the sample is uniform, the entire surface is oxidised, no hydrogen is absorbed by the cladding. As a result, the calculated generated hydrogen and the measured released hydrogen could be compared, giving an estimate for absorbed hydrogen. The difference between the two results is the absorbed hydrogen, with an average value of 65.6 cm^3. It is comparable with the result in Figure 7: an integrated estimate of the absorbed hydrogen for the 100 mm long middle section of the rod (density of the cladding tube is 0.119 g/mm) is 70.5 cm^3.

4. Conclusions

Post-test examinations were carried out to obtain data regarding the effects of oxidation and secondary hydriding on VVER claddings. The examinations covered the characterisation of geometry after the ballooning and burst, ductility, oxidation and hydrogen absorption. Oxide layer formed on the samples, with increasing thickness near the thermal centre. Due to burst the inner surface was oxidised as well. However due to the geometry and flow characteristics the inner oxide was not formed along the entire length of the cladding. The hydrogen produced from steam could penetrate the metal at positions where there was less oxide on the inner surface near the burst section, this caused the measured double-peak in the axial hydrogen distribution. Oxidation and hydrogen uptake then caused embrittlement of the cladding, weakening it near the rupture.

The results were evaluated by simulations, making it possible to estimate expected values of oxidation. The measured data will be published in the next issue of the ‘Experimental database of E110 cladding exposed to accident conditions’ included in the International Fuel Performance Experiments (IFPE) database of the OECD NEA [9], and it can be used for validation purposes and model development.

Acknowledgments

The secondary hydriding tests were supported by the Paks Nuclear Power Plant, Hungary.

The present work was supported by the National Research, Development and Innovation Fund of Hungary (contract number: NVKP_16-1-2016-0014).

References

[1] S. A. Nikulin, V. G. Khanzhin, A. B. Rozhnov, V. A. Belov, E. V. Li, Crack resistance of zirconium cladding pipes after high-temperature oxidation, Met. Sci. Heat Treat. 55 (2013) 1-2. (English translation) https://doi.org/10.1007/s11041-013-9589-5

[2] H. Uetsuka, T. Furuta, S. Kawasaki, Zircaloy-4 cladding embrittlement due to inner surface oxidation under simulated loss-of-coolant condition, J. Nucl. Sci. and Tech. 18:9 (1981) 705-717. DOI: 10.1080/18811248.1981.9733309

[3] L. Yegorova, K. Lioutov, N. Jouravkova, A. Konobeev, V. Smirnov, V. Chesanov, A. Goryachev, Experimental study of embrittlement of Zr-1%Nb VVER cladding under LOCA-relevant conditions, NUREG/IA-0211, (2005)

[4] A. Couet, A. T. Motta, R. J. Comstock, Hydrogen pickup measurements in zirconium alloys: Relation to oxidation kinetics, J. Nucl. Mater. 451 (2014) 1-13. https://doi.org/10.1016/j.jnucmat.2014.03.001

[5] J-C. Brachet, D. Hamon, M. Le Saux, V. Vandenberghe, C. Toffolon-Masclet, E. Rouesne, S. Urvoy, J-L. Béchade, C. Raepsaet, J-L. Lacour, G. Bayon, F. Ott: Study of secondary hydriding at high temperature in zirconium based nuclear fuel cladding tubes by coupling information from neutron radiography/tomography, electron probe micro analysis, micro elastic recoil detection analysis and laser induced breakdown spectroscopy microprobe, J. Nucl. Mat. 488 (2017) 267-286. https://doi.org/10.1016/j.jnucmat.2017.03.009

[6] Z. Hózer, I. Nagy, A. Vimi, M. Kunstár, P. Szabó, T. Novotny, E. Perez-Feró, Z. Kis, L. Szentmiklósi, M. Horváth, A. Pintér Csordás, E. Barsy, K. Kulacsy, M. Grosse: High-Temperature Secondary Hydriding Experiments with E110 and E110G Cladding, Zirconium in the Nuclear Industry: 18th International Symposium, ASTM STP1597, R. J. Comstock and A. T. Motta, Eds., ASTM International, West Conshohocken, PA, 2018, pp. 1093–1113, http://dx.doi.org/10.1520/STP159720160031

[7] Cs. Győri, P. Van Uffelen, A. Schubert, J. van de Laar, G. Spykman, Z. Hózer, "An Update of the Nuclear Fuel Behaviour Simulation under LOCA Conditions with the TRANSURANUS Code", KTG Technical Expert Meeting on "Status of LWR Fuel Development and Design Methods", Dresden, Germany, 2-3 March 2006. http://publications.jrc.ec.europa.eu/repository/handle/JRC33766

[8] M. Király, K. Kulacsy, Z. Hózer, E. Perez-Feró, T. Novotny, High-temperature steam oxidation kinetics of E110G cladding alloy, J. Nucl. Mater. 475 (2016) 27-36. https://doi.org/10.1016/j.jnucmat.2016.03.007

[9] E. Perez-Feró, C. Győri, L. Matus, L. Vasáros, Z. Hózer, P. Windberg, L. Maróti, M. Horváth, I. Nagy, A. Pintér-Csordás, T. Novotny, Experimental database of E110 cladding exposed to accident conditions, J. Nucl. Mater. 397 (2010) 48-54. https://doi.org/10.1016/j.jnucmat.2009.12.005

[10] M. S. Veshchunov, V. E. Shestak, Modeling of Zr alloy burst cladding internal oxidation and secondary hydriding under LOCA conditions, J. Nucl. Mater. 461 (2015) 129-142. https://doi.org/10.1016/j.jnucmat.2015.03.006

[11] W. Wiesenack: Accident-related fuel experiments in Halden - HRP LOCA Test Series IFA-650, IAEA, TWGFPT Orientation 24 April 2014,

[12] Peter Askeljung, Johan Flygare, Daniele Minghetti, “NRC LOCA Testing Programme at Studsvik, Recent Results on High Burnup Fuel”, “Transactions of TOPFUEL 2012, Manchester.

[13] D.R. Olander, “Materials chemistry and transport modeling for severe accident analyses in light-water reactors II: Gap processes and heat release, Nuclear Engineering and Design 148 (1994) 273-292”

[14] Z. Hózer, I. Nagy, N. Vér, R. Farkas: Simulation of Loss-of-Coolant Accidents in the CODEX Integral Test Facility, 40th Enlarged Halden Programme Group Meeting, 24th - 29th September, 2017, Lillehammer, paper F2.7

[15] Z. Hózer, Cs. Győri, M. Horváth, I. Nagy, L. Maróti, L. Matus, P. Windberg, J. Frecska: Ballooning Experiments with VVER Cladding, Nucl. Technology, Vol. 152, 2005, pp. 273–285.